

# Scaling patterns for azimuthal anisotropy in Pb+Pb collisions at $\sqrt{s_{NN}} = 2.76$ TeV: Further constraints on transport coefficients

Roy A. Lacey,<sup>1,\*</sup> N. N. Ajitanand,<sup>1</sup> J. M. Alexander,<sup>1</sup> J. Jia,<sup>1</sup> and A. Taranenko<sup>1</sup>

<sup>1</sup>*Department of Chemistry, Stony Brook University,  
Stony Brook, NY, 11794-3400, USA*

(Dated: April 16, 2019)

Azimuthal anisotropy measurements for charged hadrons, characterized by the second order Fourier coefficient  $v_2$ , are used to investigate the path length ( $L$ ) and transverse momentum ( $p_T$ ) dependent jet quenching patterns of the QCD medium produced in Pb+Pb collisions at  $\sqrt{s_{NN}} = 2.76$  TeV.  $v_2$  shows a linear decrease as  $1/\sqrt{p_T}$  and a linear increase with the medium path length difference ( $\Delta L$ ) in- and out of the  $\Psi_2$  event plane. These patterns compliment a prior observation of the scaling of jet quenching ( $R_{AA}$ ) measurements. Together, they suggest that radiative parton energy loss is a dominant mechanism for jet suppression, and  $v_2$  stems from the difference in the parton propagation length  $\Delta L$ . An estimate of the transport coefficient  $\hat{q}$ , gives a value comparable to that obtained in a prior study of the scaling properties of  $R_{AA}$ . These results suggest that high- $p_T$  azimuthal anisotropy measurements provide strong constraints for delineating the mechanism(s) for parton energy loss, as well as for reliable extraction of  $\hat{q}$ .

Ultrarelativistic heavy ion collisions can produce a high energy-density plasma of quarks and gluons (QGP) [1]. Full characterization of the transport properties of this plasma, is a central objective of current research at both the Relativistic Heavy Ion Collider (RHIC) and the Large Hadron Collider (LHC). A key ingredient for such a characterization is a full understanding of the mechanism by which hard scattered partons interact and lose energy in the QGP, prior to their fragmentation into topologically aligned high- $p_T$  hadrons or jets [2]. This energy loss manifests as a suppression of hadron yields [3] – termed “jet quenching” – which depends on the momenta of the partons and the path length for their propagation through the QGP [2, 4–6].

Such a suppression is routinely quantified with the measured hadron yields in A+A and p+p collisions, via the nuclear modification factor ( $R_{AA}$ ) [3, 7];

$$R_{AA}(p_T) = \frac{1/N_{\text{evt}} dN/dydp_T}{\langle T_{AA} \rangle d\sigma_{pp}/dydp_T}, \quad (1)$$

where  $\sigma_{pp}$  is the particle production cross section in p+p collisions and  $\langle T_{AA} \rangle$  is the nuclear thickness function averaged over the impact parameter ( $\mathbf{b}$ ) range associated with a given centrality selection

$$\langle T_{AA} \rangle \equiv \frac{\int T_{AA}(\mathbf{b}) d\mathbf{b}}{\int (1 - e^{-\sigma_{pp}^{inel} T_{AA}(\mathbf{b})}) d\mathbf{b}}. \quad (2)$$

The average number of nucleon-nucleon collisions,  $\langle N_{coll} \rangle = \sigma_{pp}^{inel} \langle T_{AA} \rangle$ , is usually obtained via a Monte-Carlo Glauber-based model calculation [8, 9]. Detailed measurements of the centrality and  $p_T$  dependence of  $R_{AA}$  are key to ongoing efforts to delineate the transport properties of the QGP produced in heavy ion collisions at both the LHC and RHIC [5, 6, 10–19].

Differential measurements of the azimuthal anisotropy of high- $p_T$  hadrons also provide an indispensable probe to

study jet quenching. Here, the operational ansatz is that the partons which traverse the QGP medium in the direction parallel (perpendicular) to the event plane result in less (more) suppression due to the shorter (longer) parton propagation lengths [20–23]. The resulting anisotropy can be characterized via Fourier decomposition of the measured azimuthal distribution;

$$\frac{dN}{d\phi} \propto \left( 1 + \sum_{n=1} 2v_n \cos(n[\phi - \Psi_n]) \right), \quad (3)$$

where  $v_n = \langle \cos(n[\phi - \Psi_n]) \rangle$ ,  $n = 1, 2, 3, \dots$  and the  $\Psi_n$  are the generalized participant event planes at all orders for each event. Characterization can also be made via the pair-wise distribution in the azimuthal angle difference ( $\Delta\phi = \phi_1 - \phi_2$ ) between particles [24–26];

$$\frac{dN^{\text{pairs}}}{d\Delta\phi} \propto \left( 1 + \sum_{n=1} 2v_n^a(p_T^a) v_n^b(p_T^b) \cos(n\Delta\phi) \right). \quad (4)$$

In earlier work [5, 6], we have investigated the  $p_T$  and path length ( $L$ ) dependence of jet quenching via the scaling properties of  $R_{AA}(p_T, L)$ . The observed scaling indicated a decrease of  $R_{AA}(p_T, L)$  with  $L$  and an increase of  $R_{AA}(p_T, L)$  with  $1/\sqrt{p_T}$ . These trends were shown to be compatible with an energy loss mechanism dominated by medium induced gluon radiation [4];

$$R_{AA}(p_T, L) \simeq \exp \left[ -\frac{2\alpha_s C_F}{\sqrt{\pi}} L \sqrt{\hat{q} \frac{\mathcal{L}}{p_T}} \right] \quad (5)$$

$$\mathcal{L} \equiv \frac{d}{d \ln p_T} \ln \left[ \frac{d\sigma_{pp}}{dp_T^2}(p_T) \right],$$

where  $\alpha_s$  is the strong coupling constant,  $C_F$  is the color factor and  $\hat{q}$  is the transport coefficient which characterizes the squared average transverse momentum exchange [per unit path length] between the medium and the parton. An estimate of  $\hat{q}$  was also extracted from the scaling

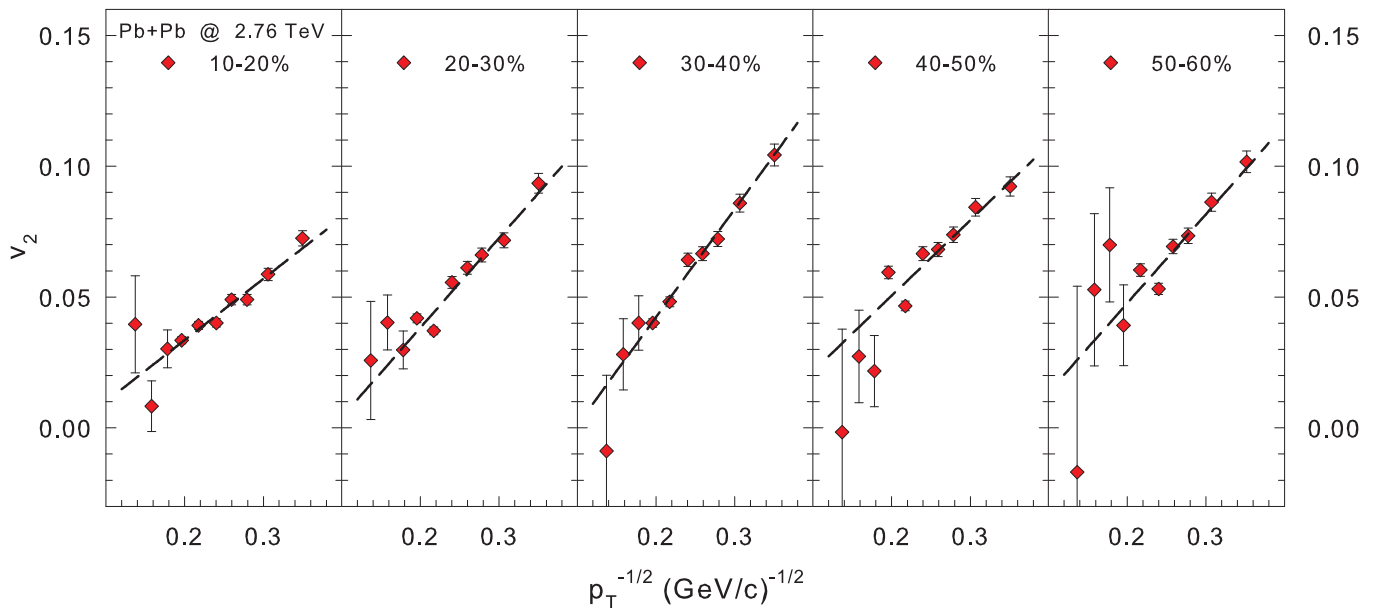


FIG. 1. (Color online)  $v_2(p_T)$  vs.  $1/\sqrt{p_T}$  for several centrality selections as indicated. Error bars are statistical only. The data are taken from Refs. [27, 28]. The dashed curve in each panel is a linear fit to the data.

61 curves. If jet quenching serves as a driver for azimuthal  
 62 anisotropy, scaling as a function of  $p_T$  and  $\Delta L = L_y - L_x$   
 63 (the difference between the out-of-plane ( $y$ ) and in-plane  
 64 ( $x$ ) path lengths) might be expected. Thus, it is impor-  
 65 tant to investigate whether azimuthal anisotropy mea-  
 66 surements show complimentary scaling patterns which  
 67 reflect the underlying energy loss mechanism suggested  
 68 by the  $R_{AA}$  measurements.

69 In this work, we use high- $p_T$   $v_2$  data to search for these  
 70 scaling patterns, with an eye toward an independent esti-  
 71 mate of  $\hat{q}$ . The observation of such patterns could also  
 72 serve as a confirmation that at high- $p_T$ ,  $R_{AA}$  and  $v_2$  stem  
 73 from the same energy loss mechanism, and this mecha-  
 74 nism is dominated by medium induced gluon radiation.

75 The high- $p_T$  ( $p_T \gtrsim 8$  GeV/ $c$ ,  $1 < |\eta| < 2$ ) measure-  
 76 ments employed in our search were recently reported for  
 77 charged hadrons by the CMS and ATLAS collaborations  
 78 [27, 28]. These data indicate an increase of  $v_2(p_T)$  from  
 79 central to mid-central collisions, as might be expected  
 80 from an increase in  $\Delta L$  as collisions become more pe-  
 81 ripheral. They also indicate a characteristic decrease of  
 82  $v_2$  with  $p_T$ , suggestive of a  $1/\sqrt{p_T}$  dependence. These  
 83 key features are important to the scaling search discussed  
 84 below.

85 To facilitate comparisons to our earlier scaling analy-  
 86 sis of  $R_{AA}$  data, we use the transverse size of the system  
 87  $\bar{R}$  as an estimate for the path length  $L$ , as was done  
 88 in our earlier analyses [5, 6]. A Monte-Carlo Glauber-  
 89 based model calculation [8, 9] was used to evaluate the  
 90 values for  $\bar{R}$  and the eccentricity  $\varepsilon$  in Pb+Pb collisions  
 91 as follows. For each centrality selection, the number of  
 92 participant nucleons  $N_{part}$ , was first estimated. Sub-

93 sequently,  $\bar{R}$  and the eccentricity  $\varepsilon$ , were determined  
 94 from the distribution of these nucleons in the transverse  
 95 ( $x, y$ ) plane as:  $1/\bar{R} = \sqrt{\left(\frac{1}{\sigma_x^2} + \frac{1}{\sigma_y^2}\right)}$ , and  $\varepsilon = \frac{\sigma_y^2 - \sigma_x^2}{\sigma_y^2 + \sigma_x^2}$ ,  
 96 where  $\sigma_x$  and  $\sigma_y$  are the respective root-mean-square  
 97 widths of the density distributions. We use the esti-  
 98 mate  $\Delta L \equiv L_y - L_x = \varepsilon(L_x + L_y) \sim \varepsilon\bar{R}$  for the path  
 99 length difference. Note that  $L_y = (\sigma_x\sqrt{1+\varepsilon})/(1-\varepsilon)$  and  
 100  $L_x = (\sigma_x\sqrt{1+\varepsilon})/(1+\varepsilon)$ . For these calculations, the ini-  
 101 tial entropy profile in the transverse plane was assumed  
 102 to be proportional to a linear combination of the number  
 103 density of participants and binary collisions [29, 30]. The  
 104 latter assures that the entropy density weighting used, is  
 105 constrained by the Pb+Pb hadron multiplicity measure-  
 106 ments [31]. Averaging for each centrality, was performed  
 107 over the configurations generated in the simulated colli-  
 108 sions.

111 Figure 1 shows the plots of  $v_2(p_T)$  vs.  $1/\sqrt{p_T}$  for sev-  
 112 eral centrality selections as indicated. The dashed curves  
 113 which represent a linear fit, indicates that within errors,  
 114  $v_2(p_T)$  decreases as  $1/\sqrt{p_T}$ . This trend is opposite to the  
 115 trend for  $R_{AA}(p_T)$ , and is to be expected if the anisotropy  
 116 characterized by  $v_2(p_T)$  stems from jet quenching (cf.  
 117 Eq. 5), *i.e.* an increase in  $R_{AA}(p_T)$  results in a corre-  
 118 sponding decrease in  $v_2(p_T)$ .

119 The combined effects of  $1/\sqrt{p_T}$  and  $\Delta L$  scaling are  
 120 demonstrated in Fig. 2. The left panel (a) of the figure  
 121 shows the same linear dependence on  $1/\sqrt{p_T}$  evidenced  
 122 in Fig. 1, but with a different magnitude for each of the  
 123 centrality selections indicated. The right panel (b) shows  
 124 that, when the same data [shown in (a)] is scaled by  $\Delta L$ ,  
 125 a single curve is obtained. The implied linear increase

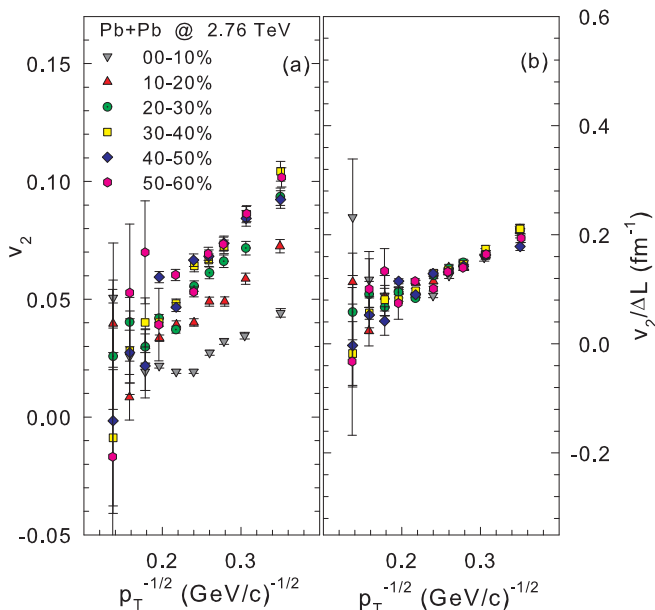


FIG. 2. (Color online) (a)  $v_2(p_T)$  vs.  $1/\sqrt{p_T}$  for the centrality selections indicated. (b)  $v_2(p_T)/\Delta L$  vs.  $1/\sqrt{p_T}$  for the same centrality selections. Error bars are statistical only.

of  $v_2(p_T)$  with  $\Delta L$  is complimentary to the previously observed  $L$  dependence of jet quenching [5, 6]. That is, an increase in the effective path length  $L$  ( $\Delta L$ ) leads to more quenching (anisotropy). An extrapolation to higher values of  $p_T$ , of a linear fit to the data in Fig. 2(b), suggests that the anisotropy associated with jet quenching is negligible ( $v_2 \sim 0$ ) for  $p_T \gtrsim 100$  GeV. This is probably due to the relatively small magnitudes of  $\Delta L$ . Note that for a fixed value of  $p_T$ ,  $\ln(R_{AA}(p_T, L))$  shows a linear dependence on  $L$  [5, 6].

For a given centrality, the azimuthal angle dependence of jet quenching [relative to the  $\Psi_2$  event plane]  $R_{AA}(\Delta\phi, p_T)$ , is related to  $v_2(p_T)$ . This stems from the fact that the number of particles emitted relative to  $\Psi_2$ ,  $N(\Delta\phi, p_T) \propto [1 + 2v_2(p_T) \cos(2\Delta\phi)]$ . The anisotropy factor

$$R_{v_2}(p_T, \Delta L) = \frac{R_{AA}(90^\circ, p_T)}{R_{AA}(0^\circ, p_T)} = \frac{1 - 2v_2(p_T)}{1 + 2v_2(p_T)}, \quad (6)$$

(i.e. the ratio of the out-of-plane yield ( $\Delta\phi = 90^\circ$ ) to in-plane yield ( $\Delta\phi = 0^\circ$ )), quantifies the magnitude of the quenching for path length difference  $\Delta L$ . Therefore, the values of  $R_{v_2}(p_T, \Delta L)$  can be used in concert with Eq. 5 to extract an estimate of  $\hat{q}$ .

To facilitate this estimate we first plot  $\ln(R_{v_2}(p_T))$  vs.  $1/\sqrt{p_T}$  for each centrality selection, as shown in Fig. 3. The dashed curve in each panel of the figure, represents a linear fit to the data; they show the expected linear dependence on  $1/\sqrt{p_T}$  predicted by Eq. 5. The slopes  $S_{p_T}$  of these curves encode the magnitude of both  $\alpha_s$  and  $\hat{q}$ .

For a given medium (fixed  $\langle\hat{q}\rangle$ ) Eq. 5 suggests that the ratio  $S_{p_T}/\Delta L$  should be independent of the collision centrality. This independence is indicated by the relatively flat centrality dependence for  $S_{p_T}/\Delta L$ , shown in Fig. 4. This observation serves as a further validation of Eq. 5, so we use the average value of these ratios  $\sim 3.0 \pm 0.3$  GeV $^{1/2}$ /fm in concert with Eq. 5, to obtain the estimate  $\hat{q}_{LHC} \approx 0.47 \pm 0.09$  GeV $^2$ /fm with values of  $\alpha_s = 0.3$  [11],  $C_F = 9/4$  [4, 32] and  $\mathcal{L} = n = 6.7$  [33]. This estimate of  $\hat{q}_{LHC}$ , which can be interpreted as a space-time average, is similar to our earlier estimate  $\hat{q}_{LHC} \approx 0.56 \pm 0.05$  GeV $^2$ /fm from scaled  $R_{AA}$  data, evaluated with the same values for  $C_F$  and  $\alpha_s$  [6]. We conclude that radiative parton energy loss drives jet suppression and a collateral azimuthal anisotropy ( $v_2$ ) develops, due to the difference in the in-medium parton propagation length ( $\Delta L$ ) in- and out of the  $\Psi_2$  event plane.

In summary, we have performed scaling tests on the  $v_2$  values obtained from azimuthal anisotropy measurements of high- $p_T$  charged hadrons in Pb+Pb collisions at  $\sqrt{s_{NN}} = 2.76$  TeV.  $v_2$  shows a linear decrease as  $1/\sqrt{p_T}$  and a linear increase with the medium path length difference ( $\Delta L$ ) in the directions parallel and perpendicular to the  $\Psi_2$  event plane. These patterns, which are similar to the scaling patterns for jet quenching measurements ( $\ln(R_{AA})$ ), confirm the  $1/\sqrt{p_T}$  dependence, as well as the linear dependence on path length predicted by Dokshitzer and Kharzeev for jet suppression dominated by the mechanism of medium-induced gluon radiation in a hot and dense QGP. These observations also suggest that, at high- $p_T$ ,  $v_2$  stems from jet quenching, and is a direct consequence of the difference in the parton propagation length  $\Delta L$ . A simple estimate of the transport coefficient  $\hat{q}$  from the scaled  $v_2$  data, gives a value which is similar to the value obtained in a prior study of the scaling properties of  $R_{AA}$  [6]. These results confirm that high- $p_T$  azimuthal anisotropy measurements, provide strong additional constraints for delineating the mechanism(s) for parton energy loss, as well as for reliable extraction of  $\hat{q}$ .

## ACKNOWLEDGMENTS

This work was supported by the US DOE under contract DE-FG02-87ER40331.A008.

\* E-mail: Roy.Lacey@Stonybrook.edu

- [1] E. V. Shuryak, Phys. Lett. **B78**, 150 (1978).
- [2] M. Gyulassy and X.-n. Wang, Nucl. Phys. **B420**, 583 (1994), arXiv:nucl-th/9306003.
- [3] K. Adcox *et al.* (PHENIX), Phys. Rev. Lett. **88**, 022301 (2002), arXiv:nucl-ex/0109003.

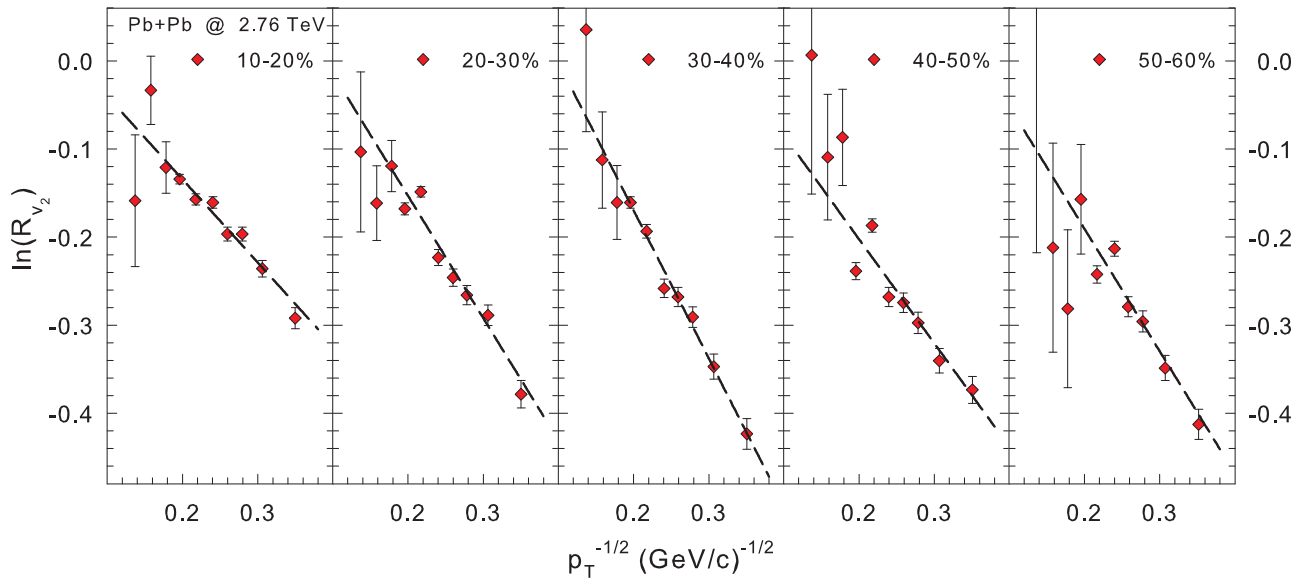


FIG. 3. (Color online)  $\ln[R_{v_2}(p_T, \Delta L)]$  vs.  $1/\sqrt{p_T}$  for several centrality selections as indicated. Error bars are statistical only. The dashed curve in each panel shows a linear fit to the data (see text).

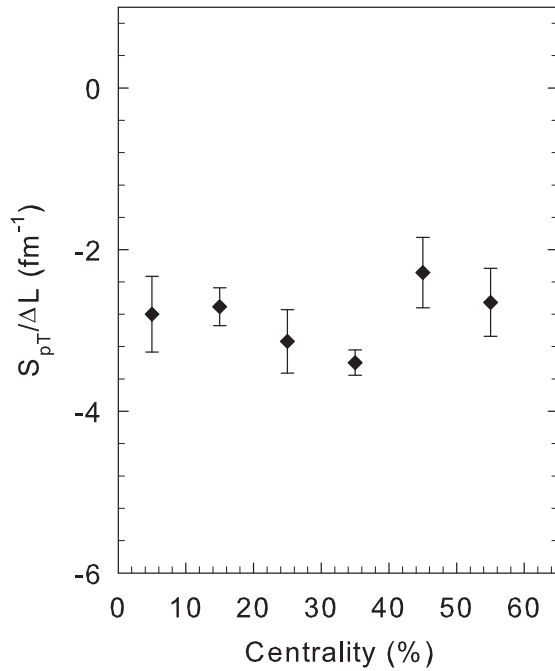


FIG. 4. (Color online) Centrality dependence of  $S_{p_T}/\Delta L$ , see text. The slopes  $S_{p_T}$  are obtained from the the linear fits shown in Fig. 3.

203 [4] Y. L. Dokshitzer and D. E. Kharzeev,  
204 Phys. Lett. **B519**, 199 (2001), arXiv:hep-ph/0106202.  
205 [5] R. A. Lacey, N. Ajitanand, J. Alexander, X. Gong, J. Jia,  
206 et al., Phys.Rev. **C80**, 051901 (2009), arXiv:0907.0168.  
207 [6] R. A. Lacey, N. Ajitanand, J. Alexander, J. Jia, and  
208 A. Taranenko, (2012), arXiv:1202.5537 [nucl-ex].

209 [7] C. Adler et al. (STAR),  
210 Phys. Rev. Lett. **89**, 202301 (2002),  
211 arXiv:nucl-ex/0206011.  
212 [8] M. L. Miller, K. Reygers, S. J. Sanders, and P. Steinberg,  
213 Ann. Rev. Nucl. Part. Sci. **57**, 205 (2007).  
214 [9] B. Alver et al., Phys. Rev. Lett. **98**, 242302 (2007).  
215 [10] G.-Y. Qin et al., Phys. Rev. Lett. **100**, 072301 (2008).  
216 [11] S. A. Bass et al., Phys. Rev. **C79**, 024901 (2009),  
217 arXiv:0808.0908 [nucl-th].  
218 [12] R. Sharma, I. Vitev, and B.-W. Zhang,  
219 Phys.Rev. **C80**, 054902 (2009), arXiv:0904.0032.  
220 [13] J. Casalderrey-Solana, J. G. Milhano, and U. A. Wiede-  
221 mann, J.Phys.G **G38**, 035006 (2011).  
222 [14] G.-Y. Qin and B. Muller,  
223 Phys.Rev.Lett. **106**, 162302 (2011).  
224 [15] T. Renk, H. Holopainen, R. Paatelainen, and K. J. Es-  
225 kola, Phys.Rev. **C84**, 014906 (2011), arXiv:1103.5308.  
226 [16] X.-F. Chen, T. Hirano, E. Wang, X.-N. Wang, and  
227 H. Zhang, Phys.Rev. **C84**, 034902 (2011).  
228 [17] A. Majumder and C. Shen, (2011), arXiv:1103.0809.  
229 [18] B. Zakharov, JETP Lett. **93**, 683 (2011).  
230 [19] B. Betz and M. Gyulassy, (2012), arXiv:1201.0281.  
231 [20] M. Gyulassy, I. Vitev, and X. N. Wang,  
232 Phys. Rev. Lett. **86**, 2537 (2001).  
233 [21] X.-N. Wang, Phys. Rev. **C63**, 054902 (2001).  
234 [22] J. Liao and E. Shuryak,  
235 Phys. Rev. Lett. **102**, 202302 (2009).  
236 [23] J. Jia, W. Horowitz, and  
237 J. Liao, Phys.Rev. **C84**, 034904 (2011),  
238 arXiv:1101.0290 [nucl-th].  
239 [24] R. A. Lacey, Nucl. Phys. **A698**, 559 (2002).  
240 [25] K. Adcox et al., Phys. Rev. Lett. **89**, 212301 (2002).  
241 [26] G. Aad et al. (ATLAS Collaboration), (2012),  
242 arXiv:1203.3087 [hep-ex].  
243 [27] CMS Collaboration, PhysicsResultsHIN11012, 2012.  
244 [28] G. Aad et al. (ATLAS Collaboration),  
245 Phys.Lett. **B707**, 330 (2012).  
246 [29] T. Hirano and Y. Nara, Phys.Rev. **C79**, 064904 (2009).

- 247 [30] R. A. Lacey, A. Taranenko, and R. Wei, (2009), 251 [32] Here, it is assumed that charged hadrons are dominantly  
248 arXiv:0905.4368 [nucl-ex]. 252 produced via the fragmentation of gluons.
- 249 [31] S. Chatrchyan *et al.* (CMS Collaboration), 253 [33]  $\mathcal{L} = n$  was determined from a power law fit to the  $p + p$   
250 JHEP **1108**, 141 (2011), arXiv:1107.4800. 254 spectrum (for  $p_T \gtrsim 8$  GeV/c) published in Ref. [34].  
255 [34] CMS (CMS Collaboration), (2012), arXiv:1202.2554.